Session VI, Pannel Discussion on Earthquake Geotechnology in Offshore Structures

SOIL-PILE INTERACTION MODEL FOR EARTHQUAKE RESPNSE ANALYSIS OF OFFSHORE PILE FOUNDATIONS

by

Toyoaki Nogami
University of California at San Diego,
La Jolla, California 92093

Second Int. Conf. on Recent Advances in Geotechnical Earthquake Engineering and Soil Dynamics, Vol. 3, St. Louis, March, 1991.

Session VI, Panel Discussion on Earthquake Geotechnology in Offshore Structures

Toyoaki Nogami
University of California at San Diego, La Jolla, California

Soil-pile interaction plays a significant role in the pile response to external loads, and is extremely complex when nonlinear conditions and dynamic conditions exist simultaneously. Furthermore, in the offshore environment, fluid motions inside and above the seabed may affect the seabed response to pile shaft motion, adding further complexity to the soil-pile interaction. Numerical models must enable to logically reproduce the complex behavior governed by various important factors. In this regard, I would like to call your attention to the following three points concerning numerical modeling of soil-pile interaction for earthquake response analysis of offshore pile foundations.

(1) Winkler Models for Dynamic Response Analysis of Pile Foundations: Various models have been used to take into account the soil-pile interaction in the dynamic response analysis of pile foundations. Among those, Winkler models are the simplest and numerically most efficient ones. However, most of those models have been developed without a logical base and thus often fail to produce the computed results consistent with mother nature. The Matlock (or Penzien) model (Matlock et al., 1978) and Novak model (Novak, 1976) may be classified as conventional Winkler models often used in the dynamic response analysis of pile foundations, while the Nogami model is a Winkler model recently developed for the dynamic and nonlinear response analysis (Nogami et al., 1983, 1985, 1987). Those three Winkler models will be discussed first herein.

The Matlock model is basically viewed as a system of a frequency-independent nonlinear spring and linear dashpot as shown in Fig. 1. The force-displacement relationship of the nonlinear spring is defined by a so-called unit load transfer curve and the dashpot is to account for the radiation damping. When a steady-state harmonic response is assumed, the force-displacement relationship of the model can be expressed in terms of a complex curve made of the real and imaginary parts. Such force-displacement relationships at two different frequencies are illustrated in Fig. 2 for $\omega_1<\omega_2$. The nonlinear spring generates both the real and imaginary parts of the force independent of frequency. The dashpot generates only the imaginary part of the force linearly proportional to frequency. The force induced in the Matlock model is summation of those spring and dashpot forces. The real part of the force generated by the Matlock model is therefore independent of frequency. The imaginary part of the force in the elastic range results entirely from the dashpot force. As displacement level increases beyond the elastic range, the imaginary part always increases due to generation of hysteresis damping in the spring.

The Novak model is limited to linear elastic conditions and steady-state harmonic motion. The model is made of a frequency dependent complex spring (Fig. 3). The stiffness of the spring is defined from the analytical formulation obtained for the vibration of an infinitely long vertical massless rigid cylinder embedded in an infinite elastic medium. Those conditions yield plane strain conditions, in which medium displacements do not vary along the vertical direction and hence body waves generated in the medium propagate only in the horizontal direction. The force-displacement relationships of the Novak model at two different frequencies are shown in Fig. 4. The model can not produce the nonlinear behavior but can do the dynamic behavior rationally for linear elastic conditions.

The Nogami model is conceptually viewed as a combination of the Matlock model and Novak model and is capable of properly producing the nonlinear behavior coupled with the dynamic behavior. The model consists of the near-field element and far-field element as shown in Fig. 5. The near-field element made of nonlinear spring and mass represents the soil right in the vicinity of the shaft. The nonlinear spring is defined by providing a static unit load transfer curve such as that used in the Matlock model (Nogami et al., 1987, 1991) and the mass is attached to produce the dynamic effects in the near-field response. The far-field element produces the effects of linear elastic behavior of the far-field soil outside the near-field. Since nonlinear response to random loading must be analyzed in the time-domain, the far-field element is modeled by frequency independent springs, dashpots and mass as shown in Fig. 5. This far-field model is developed in a rational manner from the analytical formulations of the Novak model so that it behave closely to the Novak model under the steady-state harmonic motion (Nogami et al., 1986, 1988).

When the linear elastic region of the provided unit load transfer curve is reasonable, the Nogami model behaves very closely to the Novak model except at very low frequencies as illustrated in Fig. 6a. It is noted, however, that the Novak model is based on plane strain conditions and thus does not behave realistically at those very low frequencies. Given an identical unit load transfer curve to the Nogami and Matlock models, the force-displacement relationship of the Nogami model is identical to the Matlock model under static conditions. Under dynamic conditions, however, those models behave quite differently from each other as illustrated in Fig. 6b in which two frequencies, ω_1 and ω_2, correspond to the frequencies indicated in Fig. 6a. Dynamic conditions stiffen the spring characteristics of the Nogami model in the elastic range as seen in the real part, whereas that of the Matlock model is frequency independent. Significant difference between the two model behaviors is seen in the damping (imaginary part of the curve). As stated earlier, the Matlock model increases the damping at any frequency as soil nonlinearity develops. Contrary to this, the Nogami model increases the damping at low frequencies but decreases at high frequencies. The damping results from both hysteresis damping due to nonelastic behavior and radiation damping. When nonlinearity develops in the vicinity of the shaft, the soil generates the hysteresis damping but reduces the radiation damping by reducing the energy transmitted to the far-field soil. The change in the damping due to soil nonlinearity is the net effect of those two trends. Similar behavior also are observed in the results obtained by the three-dimensional approximate nonlinear finite element analysis (Angelides and Roesset, 1981).

(2) Improved Soil-Pile Interaction Model: When the Winkler model parameters are defined simply assuming the body waves propagating only in the horizontal direction (i.g. plane strain conditions for cylindrical waves), the model generally fails to produce meaningful results at very low frequencies including the static case. This is illustrated in Fig. 7. The figure shows variations of the stiffnesses of end-bearing piles for two different thicknesses of the homogeneous soil stratum: the broken and solid lines show respectively the stiffnesses computed by using this Winkler soil-pile interaction model and using a more rigorous model with a three-dimensional continuous medium representation of the soil. Despite errors observed in the figure, when earthquake free-field motions do not contain a significant energy at frequencies below the fundamental frequency, the Winkler model based on horizontally propagating body waves may predict the behavior reasonably well in general. This is because earthquake motions are random motions containing various frequency components and the input earthquake inertia force is proportional to square of frequency. Significant concentration of the seismic energy around the fundamental resonant frequency of the stratum may also make the situation favorable for the Winkler model based on horizontally propagating body waves. However, components of motions at frequencies lower than the fundamental resonant frequency of the ground may be very important in some cases. This may be so when earthquake free-field motions contain a significant energy at frequencies below the fundamental resonant frequency of the ground and/or when the period of a soil-structure system is very long. If this is the case, the Winkler model with the parameters defined assuming

horizontally propagating body waves may not be suitable for the earthquake response analysis. It is therefore desirable to have a simple logical soil-pile interaction model which can be applicable even for frequencies below the fundamental resonant frequency of the ground.

Figure 8 shows a soil-pile interaction model which behaves well at any frequency. The model consists of springs and shear elements with mass. The springs are coupled through the shear force induced at the shear elements . The soil-structure interaction force, p, is then described as

$$p = -N\frac{\partial^2 u}{\partial z^2} + Ku + M\ddot{u}$$

where N, M and K = model parameters defining the stiffness and mass of the shear element and stiffness of the spring, respectively; and u and $\ddot{u}$ = displacement and acceleration, respectively. This is a simplified version of the model previously developed by Nogami (1990) and its model parameters can be determined through logical consideration based on continuum mechanics. With this method the values, $K\text{-}\omega^2M$ and N, are computed at various frequencies for a harmonic lateral force applied at the pile head. The computed results are shown in Fig. 9 together with the conventional Winkler model stiffness. A plane strain two-dimensional soil-pile system is considered for convenience and thus the pile shown in Fig. 9a is infinitely long in the direction perpendicular to the cross section view shown in the figure. The Winkler model stiffness for this problem, k, is expressed as $k = i\omega(\lambda + 2G)/v_p$ if the parameters are defined assuming horizontally propagating body waves in a similar manner as those defined in the Novak model: in which λ and G = Lame's constants , v_p = P-wave velocity, ω = frequency and $i = \sqrt{-1}$. It is noted that waves in this case are plane waves instead cylindrical waves. As shown in the figure, the model has the static stiffness and $K\text{-}\omega^2M$ approaches to the conventional plane strain Winkler model stiffness as frequency increases. The imaginary part appears at frequencies higher than the fundamental resonant frequency of the ground. Those are all consistent with mother nature.

<u>(3) Effects of Fluid Inside and Above Seabed</u>: The offshore environment is characterized by the existence of a fluid inside and above the seabed. If this environment affects the dynamic soil-pile interaction to a great degree, it must be taken into account appropriately in numerical soil-structure interaction models including soil-pile interaction models. In order to examine the effects of such environment, the dynamic response of a vertical massless pile, subjected to a harmonic lateral force at its head, is

computed for three cases by using the thin layer element method formulated for a fluid-saturated elasto-porous medium (Nogami and Kazama, 1992). The seabed profile along the depth and three cases considered are shown in Fig. 10. The plane strain condition is assumed: i.g. the pile is infinitely long in the direction perpendicular to the cross view shown in Fig. 10. Figure 11 shows the computed amplitude of the lateral displacement of the pile at the head. As is seen in the figure, a fluid both inside and above the seabed can affect relatively significantly the soil-pile interaction and thus the dynamic response of pile foundations. Therefore we may have to take into account the effects of a fluid both inside and above the seabed in a numerical modeling of the soil-pile interaction for the dynamic response analysis of offshore pile foundations.

REFERENCES

Angelides, D. and Roesset, J.M. (1981), "Nonlinear Lateral Dynamic Stiffness of Piles," J. Geotech. Engrg., ASCE, Vol. 107, No. 11:

Matlock, H., Foo, S.H., and Bryant, L.-L. (1978), "Simulation of Lateral Pile Behavior," Proc. Earthq. Engrg. and Soil Dyn, ASCE, Pasadena, Calf., July: 600-619.

Nogami, T. and Konagai, K. (1986), "Time-Domain Axial Response of Dynamically Loaded Single Piles," J. Engrg. Mech, ASCE, Vol. 112, No. 2: 147-160.

Nogami, T. and Chen, H.L. (1987), "Prediction of Dynamic Lateral Response of Nonlinear Single Pile by Using Winkler Soil Model," Proc. Session on Dynamic Response of Pile Foundations - Experiment, Analysis, and Observation, Geotechnical Special Publication No. 11, ASCE, Atlantic City, New Jersey, April: 39-52.

Nogami, T. and Konagai, K. (1988), "Time-Domain Flexural Response of Dynamically Loaded Single Piles, " J. Engrg. Mech, ASCE, Vol. 114, No. 9: 1512-1525.

Nogami, T. (1990), "Simplified Mechanical Subgrade Model for Dynamic Response Analysis of Shallow Foundation," J. Earthq. Engrg. and Structl. Dyn., John Wiley & Sons, Vol. 19: 1041-1055.

Nogami, T., Otani, J., Konagai, K., and Chen H.-L. (1991), "Nonlinear Soil-Pile Interaction Model for Dynamic Lateral Motion," J. Geotech. Engrg., ASCE, to appear.

Nogami, T. and Kazama. M. (1992), "Dynamic Reponse Analysis of Submerged Soil by Thin Layer Element Method," Int. J. Soil Dynamics and Earthq. Engrg., to appear.

Novak, M. (1975), "Dynamic Stiffness and Damping of Piles," J. Can. Geotech. Engrg., NRC of Canada, Vol. 11, No. 5: 574-698.

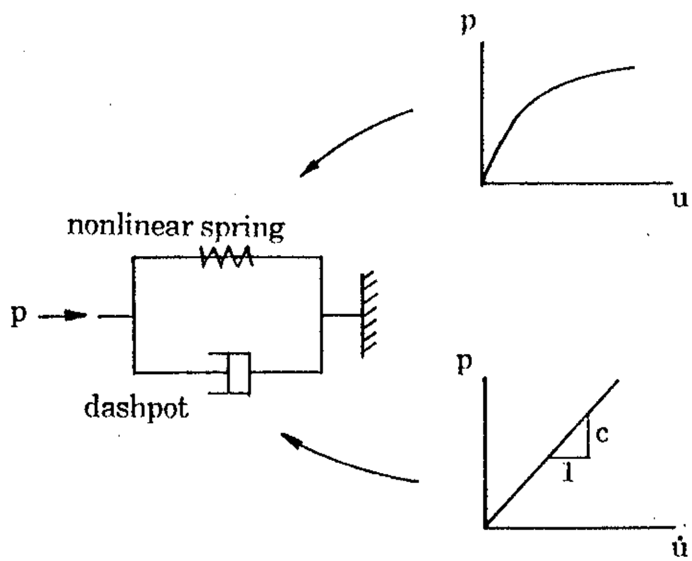

Fig. 1 Matlock Model

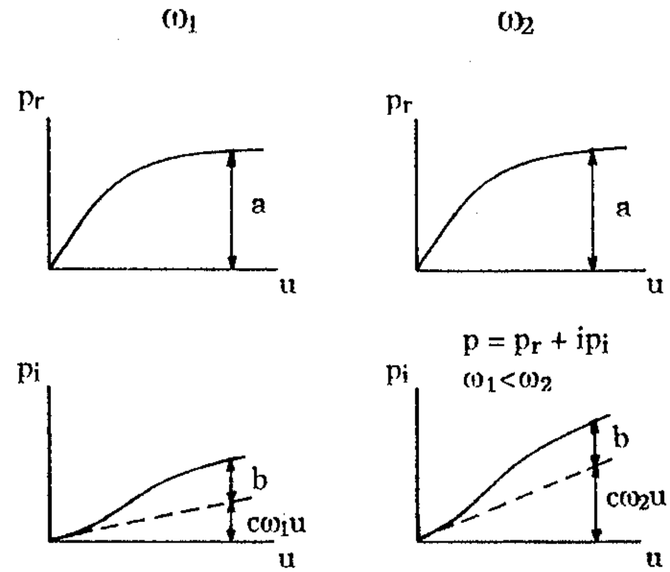

Fig. 2 Force-Displacement Relationship of Matlock Model

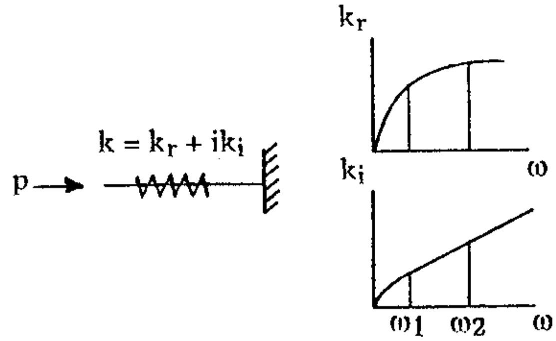

Fig. 3 Novak Model

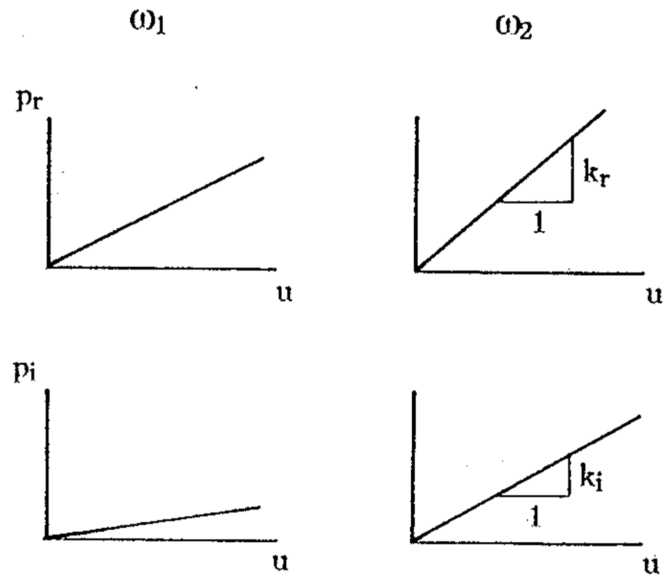

Fig. 4 Force-Displacement Relationship of Novak Model

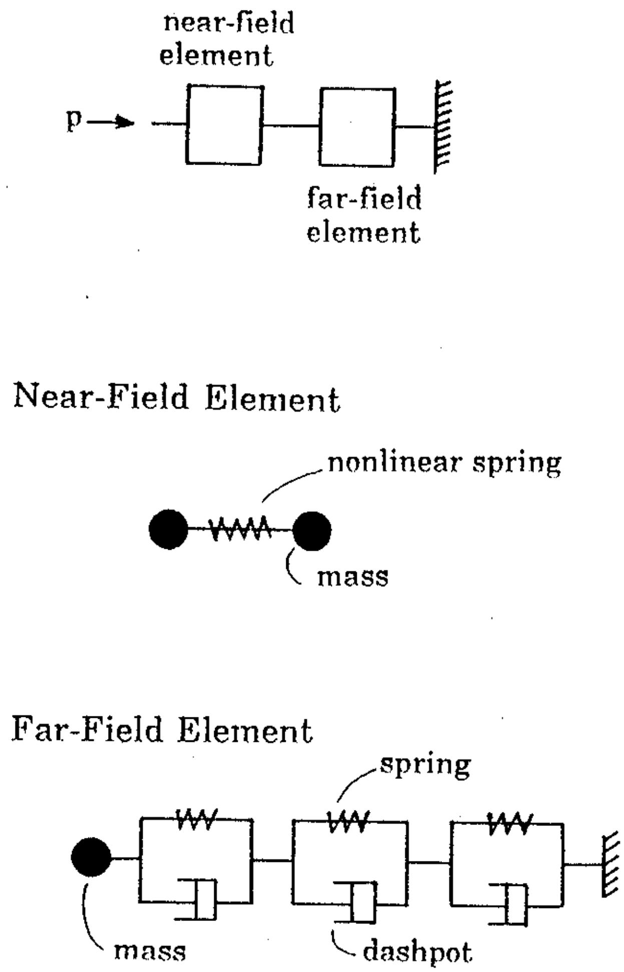

Fig. 5 Nogami Model

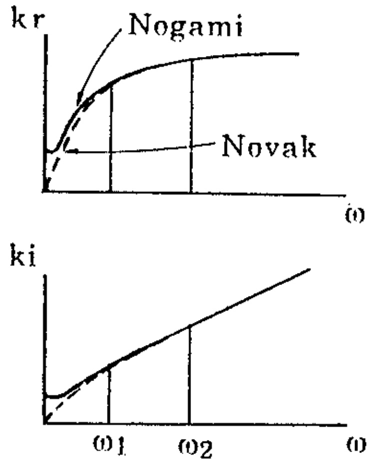

(a) Linear Elastic Conditions

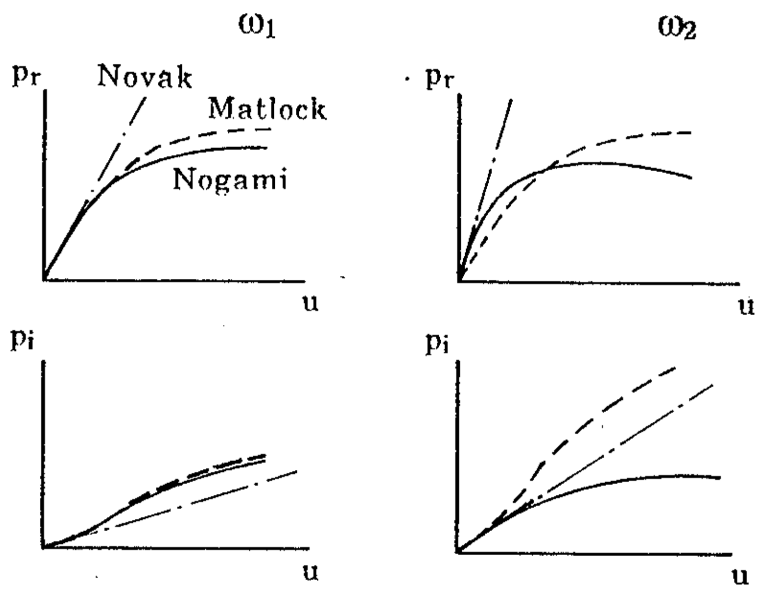

(b) Inelastic Conditions

Fig. 6 Force-Displacement Relationship of Nogami Model in Comparison with Other Models

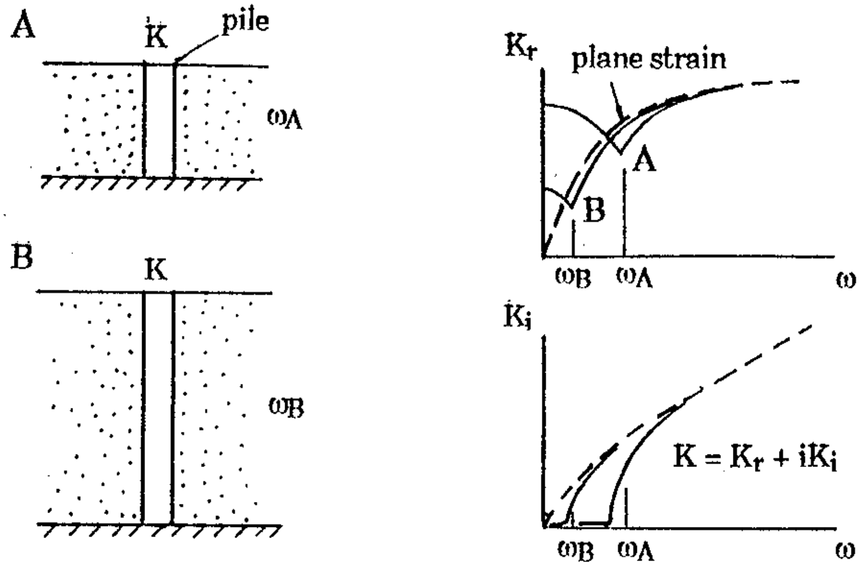

Fig. 7 Pile Stiffnesses Computed by Using Winkler Model Based on Plane Strain Conditions

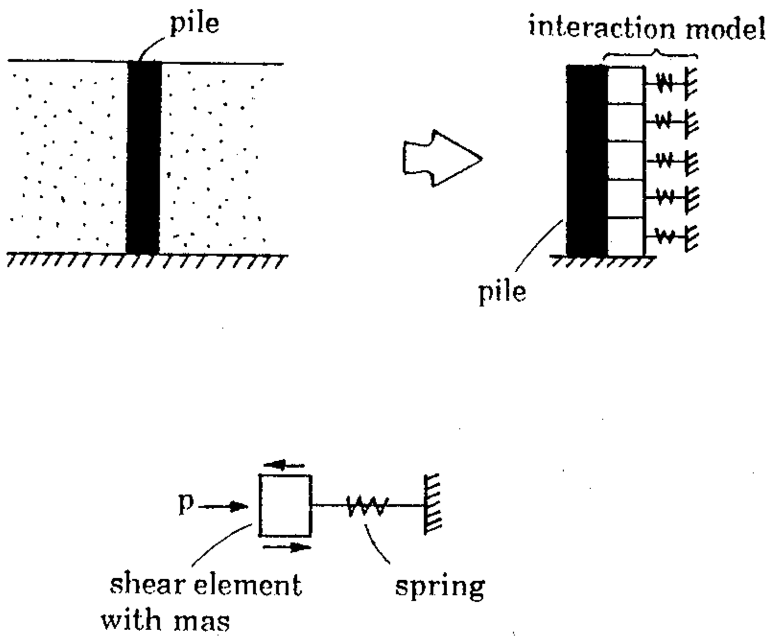

Fig. 8 Improved Model

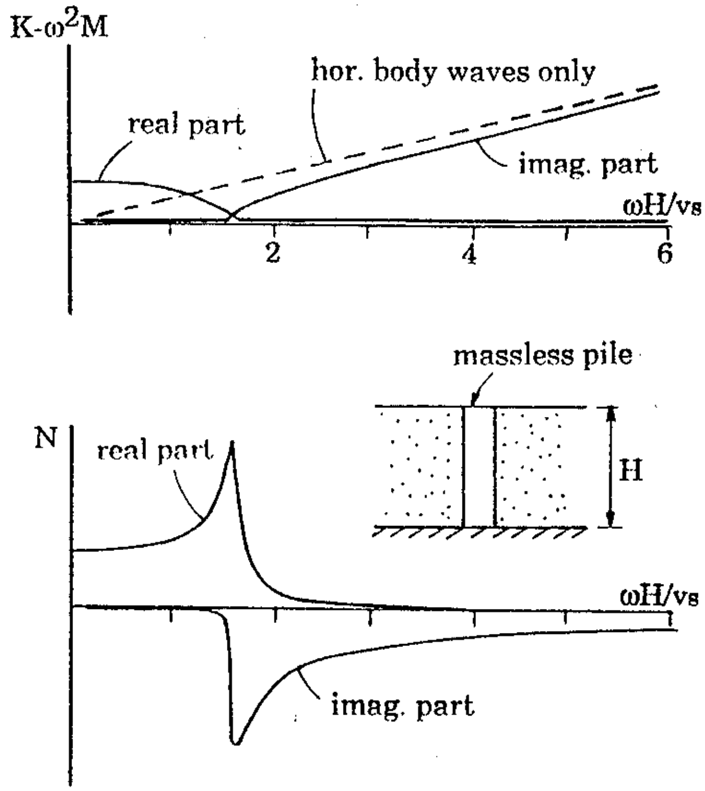

Fig. 9 Model Parameters of Improved Model Computed for Vibration of Massless Pile in Homogeneous Soil

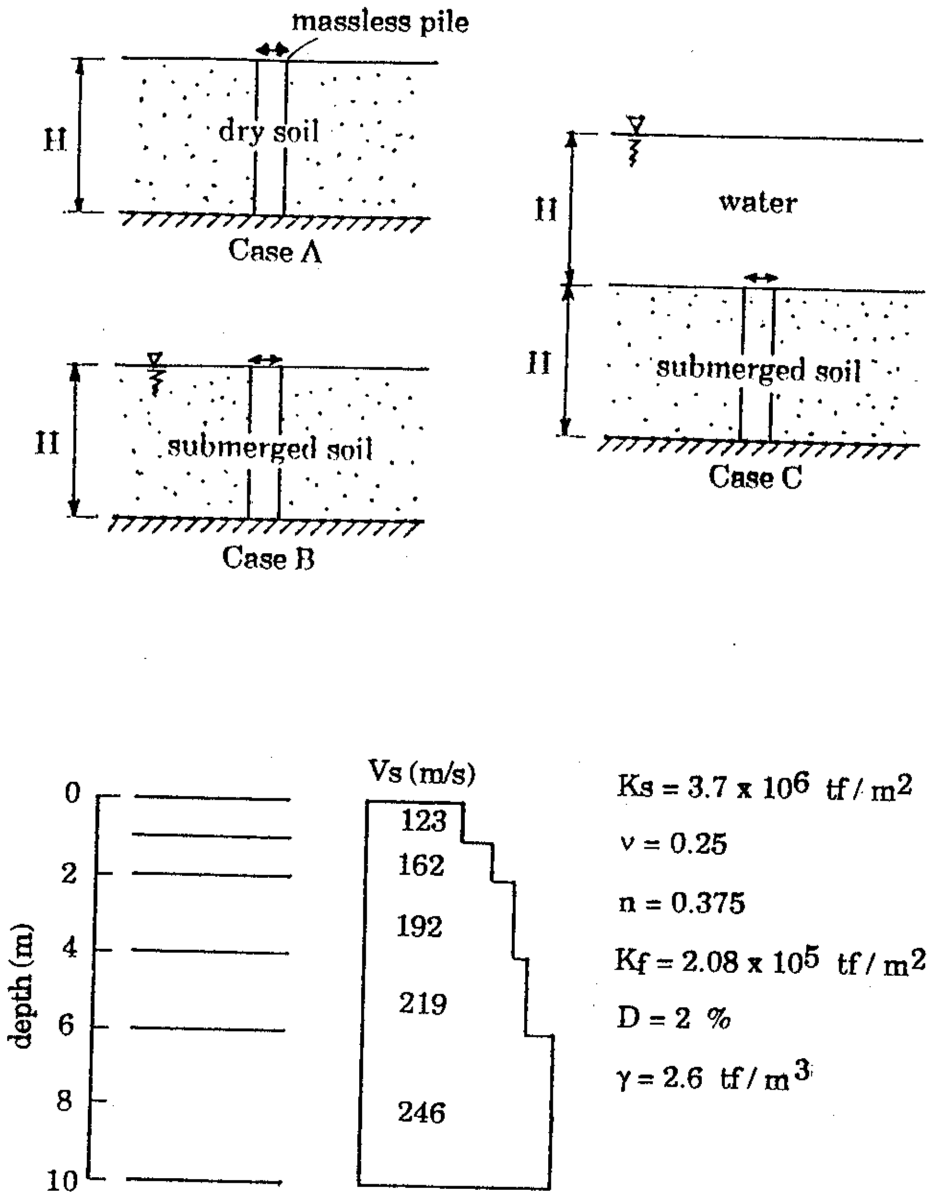

Fig. 10 Soil Profile and Three Different Cases Considered

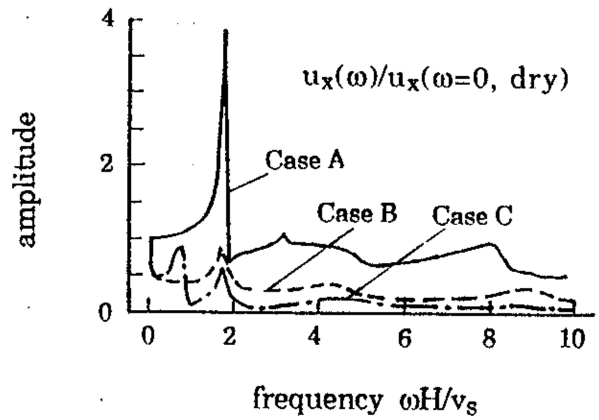

Fig. 11 Displacement Amplitudes of Pile Head for Three Different Cases